Supplement of "Wind and Wave effects on the dispersal of the Pearl River-derived sediment over the Shelf"

Guang Zhang[1,2,3], Suan Hu[1,2,3], Xiaolong Yu[1,2,3], Heng Zhang[1,2,3], Wenping Gong[1,2,3]*

[1] School of Marine Sciences, Sun Yat-sen University, Guangzhou, China, 510275

[2] Guangdong Provincial Key Laboratory of Marine Resources and Coastal Engineering, Guangzhou 510275, China

[3] Pearl River Estuary Marine Ecosystem Research Station, Ministry of Education, Zhuhai 519082, China

*Corresponding author: Wenping Gong (gongwp@mail.sysu.edu.cn)

Model validations

The model performance was quantified using several metrics including mean bias, root-mean-square error (RMSE), and model skill (Willmott, 1981). Bias in model validation refers to the consistent deviation between model predictions and observed data, indicating whether the model tends to overestimate or underestimate certain variables compared to actual measurements. The RMSE quantifies the average deviation between the model results and the observations. It provides a measure of the overall accuracy of the model's predictions. Model skill represents the agreement between the model and the observations. A model skill value of 1 indicates perfect agreement between the model and the observations, while a value of 0 indicates complete disagreement. The model skill is calculated as follows:

$$\mathrm{SK} = 1 - \frac{\sum_{i=1}^{N} |X_{mod} - X_{obs}|^2}{\sum_{i=1}^{N} \left(|X_{mod} - \overline{X}_{obs}| + |X_{obs} - \overline{X}_{obs}| \right)^2} \tag{1}$$

where X_{obs} and X_{mod} are the observation and model results, respectively, $\overline{X}_{obs}$ indicates the average data and N is the number of observations.

The modeled water levels and non-tidal levels were compared against yearlong observations at the Quarry Bay water level station (Figure S1a-b). Throughout this period, semidiurnal and weaker diurnal tides were prevalent in the PRE. Notably, significant variation at the spring/neap cycle was observed, with the tidal range fluctuating from less than 1 meter during neap tides to greater than 2 meters during spring tides. The modeled water levels exhibit good agreement with observed water levels, with RMSE of less than 0.13 m and skill values exceeding 0.98. Additionally, the predictions of non-tidal water levels demonstrate strong agreement with observations, characterized by RMSE values of less than 0.11 m and skill values exceeding 0.91. Wave data collected at W station (Figure 1b) from November 1 to December 31, 2009, were compared with simulated significant wave heights (Figure S1c). The model showed strong agreement with observations, with a skill value exceeding 0.93 and a RMSE below 0.29 m.

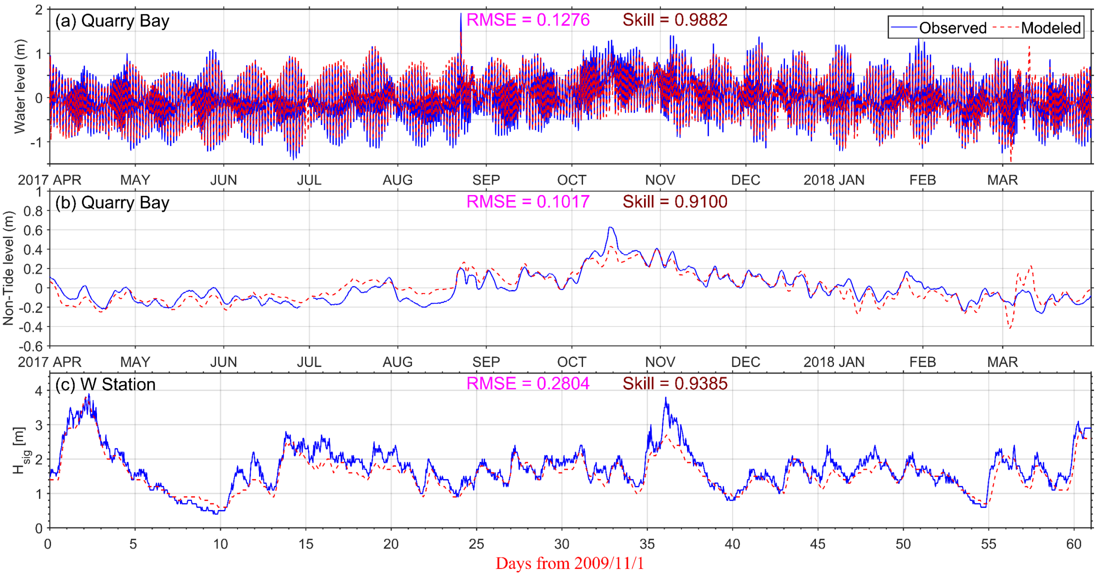

Figure S1. The validations of (a) water level, (b) non-tide level at Quarry Bay, and significant wave height at W station.

From August 16 to 21, 2017, Liu et al. (2023) conducted a continuous 115-hour onboard observation at S1 station in the PRE (Figure 1b) and obtained data such as flow velocity, salinity, and SSC. We utilized these publicly available data to validate our model, as depicted in Figure S2. The flow velocity validation demonstrates excellent agreement, with minimal bias and RMSE, and a skill value exceeding 0.9. Salinity validation also exhibits relatively good performance, with a small bias and a skill value of 0.87. However, the RMSE exceeding 4 psu suggests that the accuracy of the seabed topography may be limited. The validation of SSC produces reasonably good results, with a small bias indicating accurate magnitude in the model simulation. Nevertheless, the RMSE of 30.4 mg L^{-1} suggests a slight deficiency in the model's ability to replicate SSC variations over time. Nonetheless, the skill value of 0.84 indicates that the model results remain well representative of the observed data.

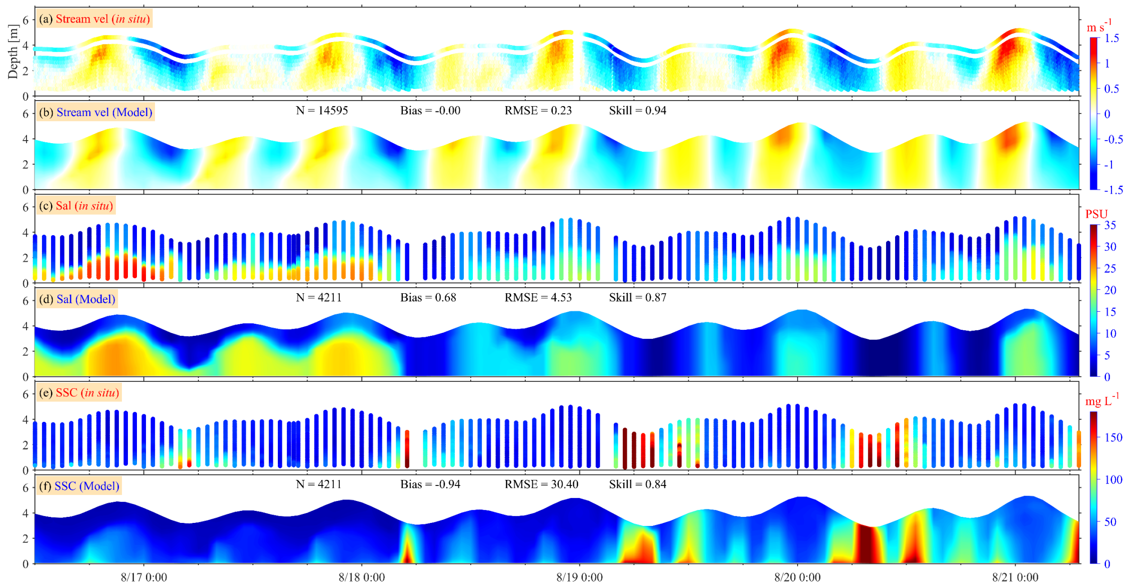

Figure S2. The validations of flow velocity, salinity, and suspended sediment concentration (SSC) of seawater at station S1, whose location is shown in Figure 1. Rows 1, 3, and 5 display the observed data, while Rows 2, 4, and 6 showcase the corresponding model results.

From August 1st to 7th, 2017, Sun Yat-sen University (SYSU) conducted a voyage campaign that covered the PRE and its adjacent waters on the inner shelf (Figure 1b), from onboard the R/V Changhe Ocean (Chen et al., 2019; Zhang et al., 2021). During this period, CTD (Conductivity, Temperature, Depth) data were collected at 43 stations. These CTD measurements provided temperature and salinity profiles at various depths for each station. Additionally, surface water samples were taken and filtered to obtain SSC in the surface layer. These field data were collected to verify the accuracy of the model's predictions of salinity, temperature, and SSC.

Figure S3 presents the comprehensive validation results of salinity, temperature, and SSC at 43 stations during the SYSU campaign. Salinity validation exhibits excellent agreement, with a bias of merely 0.34 psu, an RMSE of 2.17 psu, and a skill value of 0.98. Temperature validation also shows relatively good performance, with both bias and RMSE at 1 degree Celsius, along with a skill value of 0.89. The validation of SSC yields reasonably good results. The small bias suggests an accurate magnitude in the model simulation. However, the RMSE of 7.65 mg L^{-1} indicates a slight deficiency in the model's capability to reproduce SSC variations over space. Nevertheless, the skill value of 0.74 indicates that the model results remain well representative of the observed data.

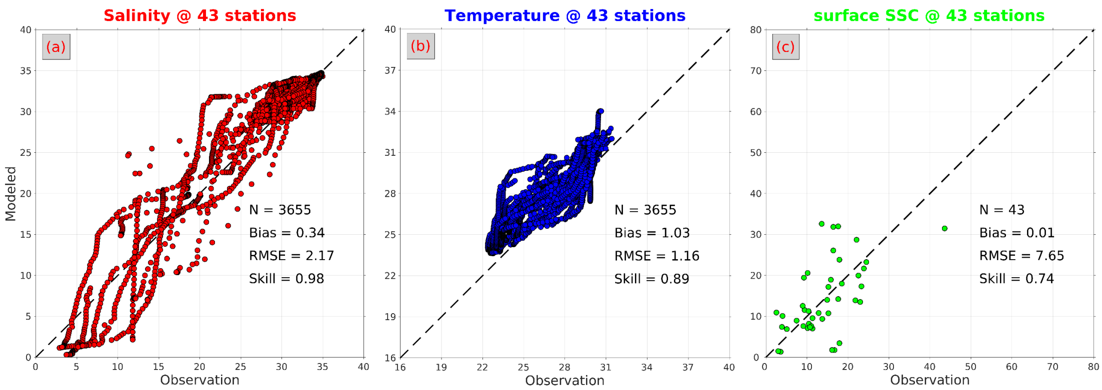

Figure S3. The validations of (a) salinity, (b) temperature, and (c) SSC at the 43 stations during the 2017 SYSU campaign.

Supplementary model results analysis

In No wind or wave case, the water level is higher in the PRE and western coast. The nearshore areas to the east of the estuary have lower water levels, with higher levels offshore (Figure S4a), forming a cross-shore water level gradient (Figure S4e). This corresponds to the region experiencing upwelling driven by strong tidal currents and topographic interactions (Gan et al., 2009). When the river plume expands outward, it encounters upwelling and is transported eastward on the southern side of the upwelling, resulting in lower water density in the expansion area (Figure S4c). This further exacerbates the cross-shore density gradient in the area (Figure S4g), forming a transport belt moving eastward (Figure S4o).

In Wind and wave case, water levels accumulate along the PRE and western coast (Figure S4b), consistent with Yang et al. (2002). The accumulated water levels are even higher compared to No wind or wave case. The nearshore areas to the east of the estuary experience lower water levels under the summer southwest monsoon and higher water levels due to strong northeast winds in winter, resulting in overall higher water levels than No wind or wave case (Figure S4b). Due to wind and wave effects, the annual average river plume mainly transports westward from the estuary (Figure 7a), with higher surface densities to the east of the estuary and smaller cross-shore density gradients (Figure S4h). The nearshore areas to the west of the estuary exhibit a pattern of lower nearshore and higher offshore densities with density fronts (Figure S4d and S4h). A westward transport belt forms offshore (Figure S4p). In Wind and wave case, bottom shear stress mainly increases in shallow areas on both sides out of the PRE (black dashed boxes in Figure S4m-n), corresponding to an increase in turbulent kinetic energy (TKE) in those areas (Figure S4k-l).

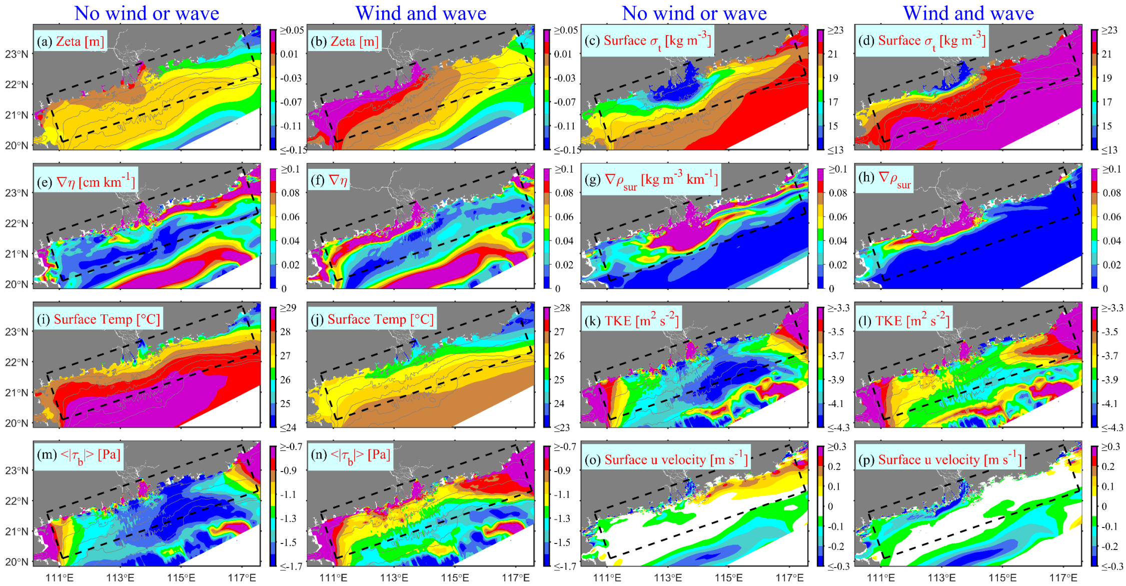

Figure S4. Annually averaged patterns of (a-b) water level, (c-d) surface density anomaly, (e-f) water level gradient, (g-h) surface density gradient, (i-j) surface temperature, (k-l) logarithm of TKE, (m-n) logarithm of bottom stress magnitude, (o-p) surface velocity in x-axis direction. No Wind or wave (Columns 1 and 3) and Wind and wave (Columns 2 and 4) scenario, respectively.

References

Chen, Y., Chen, L., Zhang, H., Gong, W., 2019. Effects of wave-current interaction on the Pearl River Estuary during Typhoon Hato. Estuarine, Coastal and Shelf Science 228, 106364.

Gan, J., Cheung, A., Guo, X., Li, L., 2009. Intensified upwelling over a widened shelf in the northeastern South China Sea. Journal of Geophysical Research 114.

Liu, H., Ye, L., Zhou, W., Wu, J., 2023. Salt-wedge intrusion-retreat cycle induced sediment floc dynamics in bottom boundary layer (BBL) of a micro-tidal estuary. Marine Geology 466, 107175.

Willmott, C.J., 1981. On the Validation Of Models. Physical Geography 2, 184-194.

Yang, H., Liu, Q., Liu, Z., Wang, D., Liu, X., 2002. A general circulation model study of the dynamics of the upper ocean circulation of the South China Sea. Journal of Geophysical Research: Oceans 107.

Zhang, H., Hu, S., Cheng, W., Zhu, L., Chen, Y., Liu, J., Gong, W., Li, Y., Li, S., 2021. Response of freshwater transport during typhoons with wave-induced mixing effects in the Pearl River Estuary, China. Estuarine, Coastal and Shelf Science 258, 107439.